Materials Transactions, Vol. 45, No. 8 (2004) pp. 2723 to 2727

Phase Selection in Undercooled $Y_3Al_5O_{12}$ Melt

Kosuke Nagashio*[1], Jun Sasaki*[2] and Kazuhiko Kuribayashi

Institute of Space & Astronautical Science, Japan Aerospace Exploration Agency, Sagamihara 229-8510, Japan

Two kinds of solidification paths from $Y_3Al_5O_{12}$ melt has been reported; one is stable $Y_3Al_5O_{12}$ (YAG) garnet, the other is metastable $YAlO_3$ perovskite (YAP) and subsequent YAP+Al_2O_3 eutectic. The reason for this, however, has been puzzled. The effect of cooling rate on this phase selection was addressed under containerless condition using an aero-acoustic levitator. A high-speed video camera (HSV) enabled us to directly observe the recalescence behavior. As the cooling rate increased from 15 to 350 K/s, the solidification of a metastable YAP and YAP+Al_2O_3 eutectic, a monophasic YAG, and an amorphous phase were successively obtained. At around the critical cooling rate of approximately 50 K/s for the formation of YAP and YAG, simultaneous recalescence of YAP and YAG was observed by HSV, and the sample obtained contained both the metastable YAP and stable YAG. The nucleation rate of YAG corresponds with that of YAP at the critical cooling rate and the growth velocity of YAP, which first nucleated in the undercooled melt, was slow enough for YAG to nucleate in the remaining undercooled melt, resulting the simultaneous recalescence. In general, the metastable phase nucleates at the higher cooling rate than the stable phase. However, in this system, the higher nucleation barrier of YAG than that of YAP led to the nucleation of YAG at the higher cooling rate.

(Received April 13, 2004; Accepted June 10, 2004)

Keywords: *$Y_3Al_5O_{12}$, phase selection, containerless solidification, cooling rate, high-speed video imaging*

1. Introduction

$Y_3Al_5O_{12}$ garnet (YAG) is technologically important laser host material[1,2] and also is known as a high-temperature strength material.[3] Many researchers have studied the crystal growth of YAG from the melt for its industrial importance. In the case of conventional solidification experiment using crucible, Caslavsky and Viechnicki[4] reported that metastable $YAlO_3$ (YAP) and subsequent YAP+Al_2O_3 eutectic were formed when the melt temperature exceeded a critical value (T_{cl}) of 2273 K, which is 60 K higher than the melting temperature ($T_M = 2213$ K) of YAG, before cooling and that YAG solidified only from the melt remained below T_{cl}. Similar results have been reported by other researchers by calorimetric analyses.[5,6]

On the other hand, Gervais *et al.*[7] have reported the rapid cooling experiment of YAG melt under containerless condition using an aerodynamic levitation furnace. They varied sample size and gas flow rate and obtained three different products with increasing undercoolings. These products were (i) a metastable mixture of YAP and Al_2O_3 crystallized at around 1600 K, (ii) YAG crystallized at around 1300 K and (iii) an amorphous phase. Although this result suggested that there did not exist T_{cl} in case of containerless processing, the criterion for phase selection in the YAG system is still open scientific subject.

The containerless processing using an aero-acoustic levitator (AAL)[8] has advantages to elucidate the criterion for phase selection in the YAG system because the difference in nucleation behavior of YAG and YAP at the crucible wall is eliminated. Moreover, free surface of the levitated droplet enables the *in-situ* observation of recalescence behavior by a high-speed video camera (HSV). Two-directional heating system from both sides of the droplet in the AAL can reduce the temperature distribution inside the melt in comparison with the aerodynamic levitation furnace technique using a conical nozzle where one-direction heating system was applied. In this study, the containerless solidification experiment was carried out to further investigate nucleation and growth behavior, especially the effect of cooling rate on phase selection in the YAG system in detail.

2. Experimental Procedure

The spherical samples were prepared by melting the powder with the $Y_3Al_5O_{12}$ composition on a water-cooled Cu hearth using a CO_2 laser irradiation. The typical specification of the spherical sample is 3.5 mm in diameter and 75 mg in weight. The melting and cooling of samples levitated in dry oxygen gas flow was performed using the AAL coupled with the CO_2 laser. The surface temperature was measured by a thermopile with broadband operating wavelength from 4.6 to 5.2 μm and a spot diameter of 2 mm, because the YAG melt is transparent in the visible range. Temperature was calibrated by the same method as reference.[9]

The samples were heated up to 2773 K, which was much higher than T_{cl} as well as T_M, and held at around 2400 K after melting. The mass loss during melting was less than 0.5%. This heating process prevents from considering the existence of T_{cl}. The molten droplets were cooled down at the cooling rates of about 15∼350 K/s by turning off or by decreasing the CO_2 laser power gradually. Once the spontaneous nucleation occurred in the undercooled melt, the laser heating was turned off immediately so that the sample was rapidly cooled down to room temperature. HSV was operated at 500 frames/s to observe the recalescence behavior of levitated droplets and also to measure the growth velocity. The phases were identified by powder X-ray diffraction (XRD). The microstructure was observed by scanning electron microscopy (SEM) in conjunction with an energy-dispersive spectroscopy (EDS).

*[1]Corresponding author

*[2]Graduate Student, The University of Tokyo, Present address: IHI aerospace

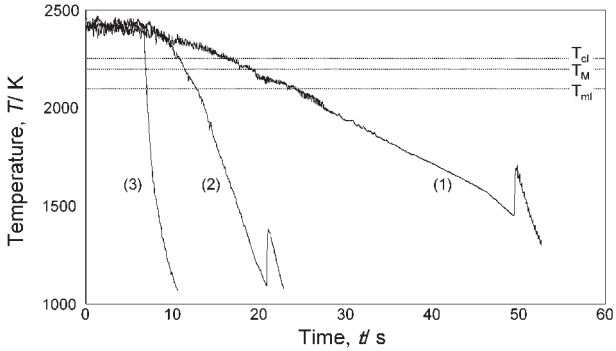

Fig. 1 Typical time-temperature profiles obtained at three different cooling rates. T_M, T_{cl}, and the metastable liquidus temperature (T_{ml}) of YAP at the $Y_3Al_5O_{12}$ composition are indicated by broken lines.

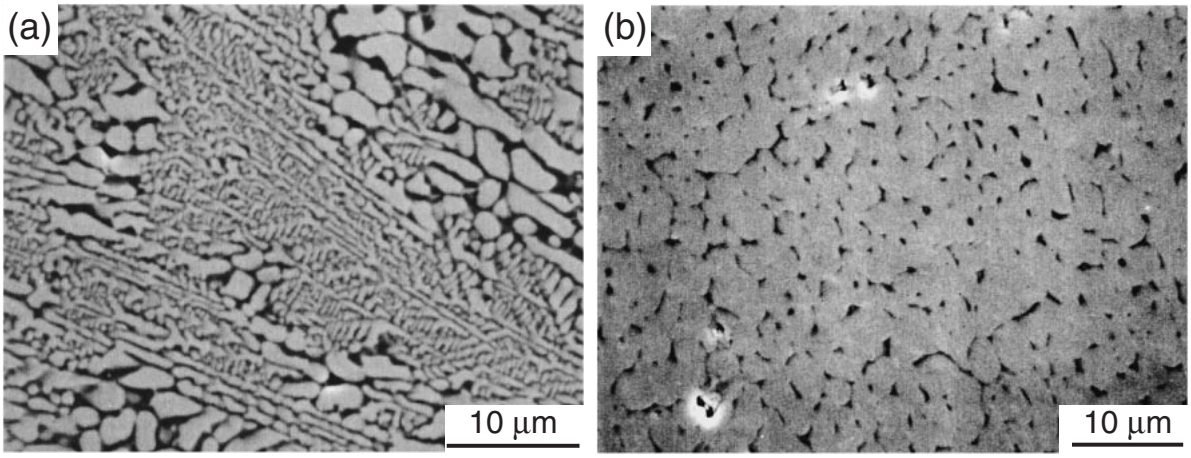

Fig. 2 SEM micrographs of polished cross sections of the processed samples. (a) This sample was obtained at low cooling rate of ~15 K/s. White YAP solidified primarily and black Al_2O_3 segregated in the interdendritic regions. (b) This sample was obtained at high cooling rate of ~150 K/s. The cellular microstructure of YAG was observed throughout the sample.

3. Results and Discussion

3.1 Effect of cooling rate on phase selection

All the melts held at around 2400 K were cooled down by turning off or decreasing the laser power. Figure 1 shows typical time-temperature profiles obtained at three different cooling rates. It is noted that the laser was cut off immediately after recalescence occurred. In the curve (1) with the lowest cooling rate of ~20 K/s, nucleation occurred at 1149 K. The curve (2) was obtained at the moderate cooling rate of ~50 K/s. In this case, nucleation temperature of 1092 K was lower than that in (1). In the curve (3) obtained at the highest cooling rate of ~250 K/s, there was no detectable temperature rise, resulting in the amorphous sample.

Figure 2 shows the SEM micrographs of polished cross sections of the processed samples. The white dendritic pattern of YAP was clearly observed in the sample obtained at low cooling rate of ~15 K/s and black Al_2O_3 segregated in the interdendritic regions, as shown in Fig. 2(a). These phases were identified by EDS and the XRD result of this sample in Fig. 3(a). Figure 2(b) shows the cellular microstructure of YAG in the sample obtained at high cooling rate of ~150 K/s and intense XRD peaks of YAG are clearly observed in Fig. 3(b).

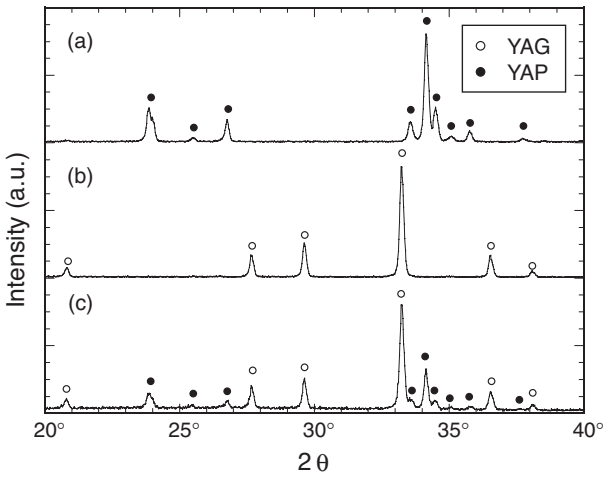

Fig. 3 XRD results for the samples obtained at different cooling rates, (a) ~15 K/s, (b) ~150 K/s, and (c) ~50 K/s.

Figures 4(a) and (b) show the HSV images of recalescence behaviors of primary YAP and YAG, respectively. The undercooled melt is dark, while growing solid is bright because of the release of the latent heat. The solid/liquid interface of YAP (a) clearly moved from upper-right side to

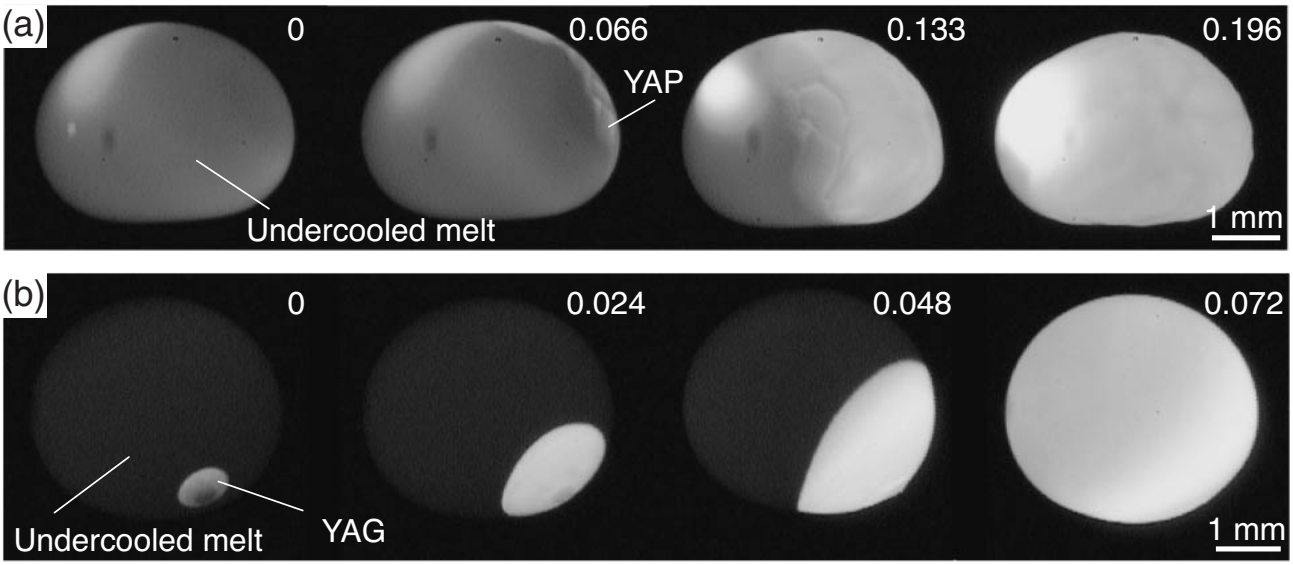

Fig. 4 HSV images of recalescence behaviors of primary YAP (a) and YAG (b). The undercooled melt is dark, while growing solid is bright because of the release of the latent heat. The elapsed time (in seconds) is indicated at the top right of the photographs.

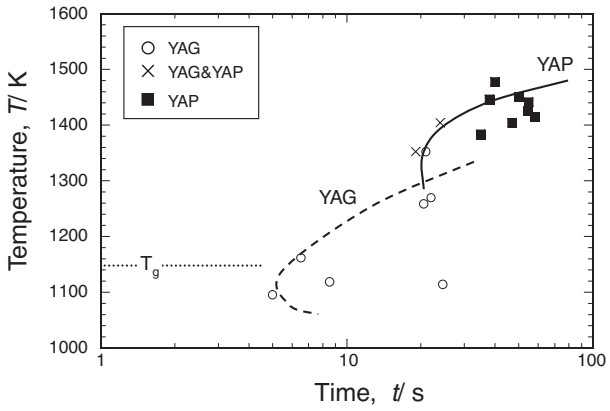

Fig. 5 Nucleation temperatures of samples obtained at different cooling rates as a function of time. The glass transition temperature in Ref. 10) is indicated in this figure.

bottom-left side of the sample. Note that the solid/liquid interface showed the peculiar pattern like carving. Moreover, the growth velocity was estimated as approximately 12 mm/s. On the other hand, the solid/liquid interface of YAG (b) was smooth. The estimated growth velocity was approximately 30∼50 mm/s that is about three or four times larger than that of YAP, because the growth of YAP requires the solute partition at the solid/liquid interface.

All the samples obtained at different cooling rates were identified by XRD and EDS. Figure 5 summarizes time vs nucleation temperature profiles where the phase identification in the sample was indicated by using different symbols. The nucleation temperatures of YAG were lower than those of YAP. The glass transition temperature line which was obtained in reference[10] is also superimposed in Fig. 5. The solidification of a metastable mixture of $YAlO_3$ (YAP) and Al_2O_3, a monophasic YAG and an amorphous phase were successively obtained from the melt heated above T_{cl}, as the cooling rate increased from 15 to 350 K/s. It is clearly seen that phase selection in the YAG system depends not on T_{cl} but on the cooling rate.

Solid and broken lines in Fig. 5 indicate the continuous cooling transformation (CCT) curves for YAP and YAG, respectively. Generally, in the metallic system, the difference in the activation energies for nucleation between the stable and metastable phases is not so large. Therefore, it is reasonable that one may need the cooling rate high enough to suppress nucleation of the stable phase in order to obtain the metastable phase, because the melting point of the stable phase is always higher than that of the metastable phase. In the present study, however, the CCT curve of stable YAG is located below that of metastable YAP. The activation energy for nucleation of YAG is much larger than that of YAP, because the garnet structure with 160 atoms in the unit cell is more complex than the perovskite structure. This seems one of main reasons for the replacement of the CCT curves.

3.2 Transition behavior at the critical cooling rate

At the critical cooling rate of ∼50 K/s between primary YAP and YAG, both YAP and YAG were often found in one sample, as shown in Fig. 3(c). The intense peaks of YAG and YAP are observed. Figures 6(a), (b) and (c) shows cross-sectional SEM images of the different parts in the processed sample containing both YAP and YAG. At the edge part (a) of the sample, primary YAP dendrites were observed and the segregation of Al_2O_3 was found in the interdendritic regions, which is similar to Fig. 2(a). At the center (b) of the sample, primary YAP dendrites were remelted by the latent heat of YAG, resulting in the transition from YAP to YAG. Finally, the cellular morphology of YAG was observed in the opposite edge part (c) of the sample. However, the primary YAP is still seen in Fig. 6(c). The successive transition from YAP to YAG occurred in one sample.

Figure 7 shows the HSV images of the sample containing both YAP and YAG. The first recalescence started from the

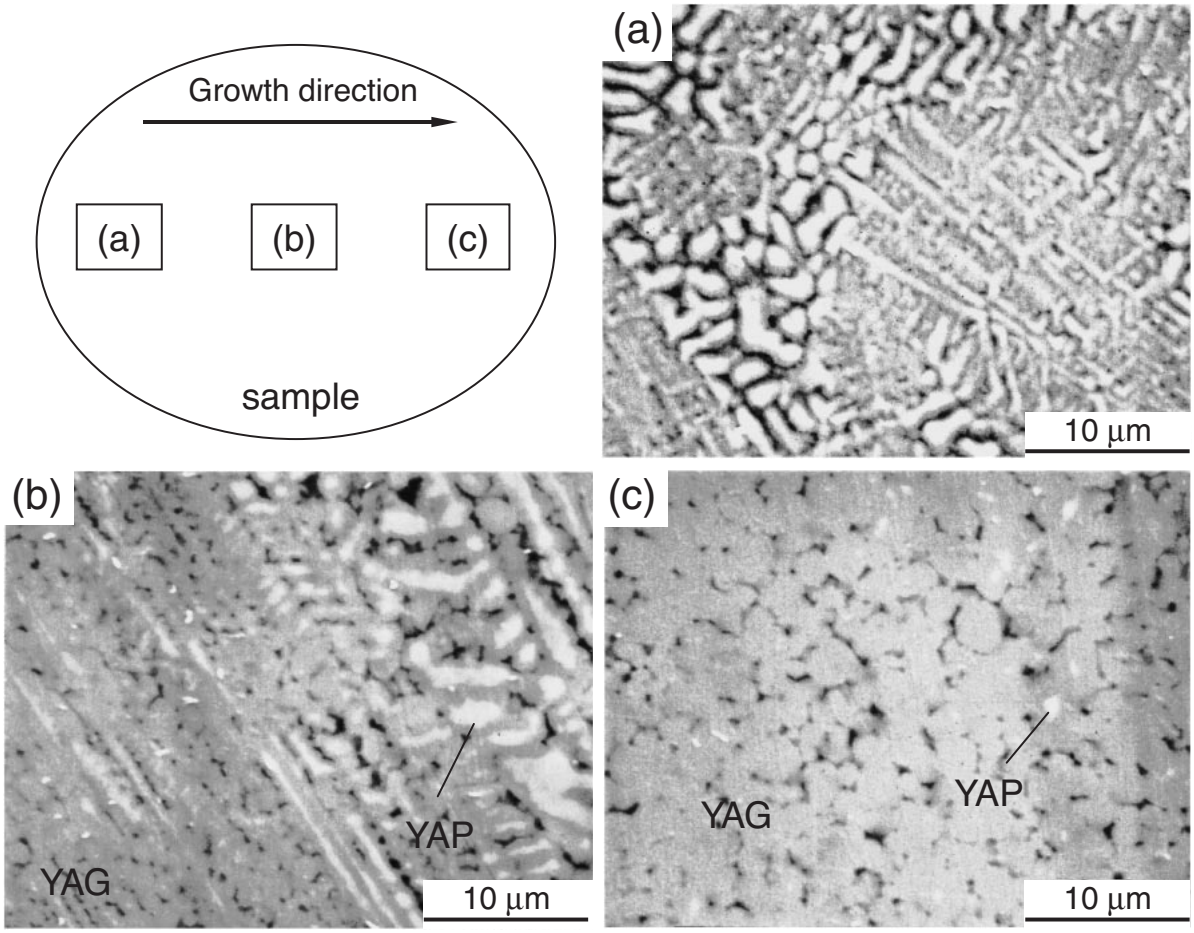

Fig. 6 Schematic illustration of the sample showing growth direction. SEM images (a), (b) and (c) are taken at positions (a), (b) and (c) in the illustration, respectively.

bottom-right side with peculiar pattern which is similar to that in Fig. 4(a). Therefore, it is reasonable that the first recalescence is ascribed to the primary solidification of YAP. And the second one which started at the upper side covered whole area of sample. This behavior is consistent with the microstructure in Fig. 6 where dendritic YAP was surrounded by YAG. Suppose that the post-recalescence temperature of YAP reaches the metastable liquidus temperature of YAP at the $Y_3Al_5O_{12}$ composition, the remaining melt still has the sufficient driving force for nucleating YAG, because the melting point of YAG is much higher than the metastable liquidus temperature of YAP. Therefore, YAG can nucleate on the primary YAP or in the remaining melt and, then, YAP is remelted by the latent heat of YAG. Strictly speaking, the mixed structure of YAP and YAG will be found under the condition that the nucleation rate of YAP is slightly higher than that of YAG because the growth velocity of YAG is much higher than that of YAP.

The transition from metastable phase to stable phase in one sample has been observed in oxide[11] and metallic[12] systems. For example, in the case of the Fe-Ni-Cr system, the transition from the metastable δ to stable γ was proved by the high speed pyrometery.[13,14] It was reported that the nucleation of the stable γ took place at the melt/δ interface. This transition has been called as double recalescence and been explained by the nucleation theory that the nucleation barrier for the metastable phase becomes smaller than that for the stable phase at a critical undercooling. Therefore, double recalescence is always observed when the melt was undercooled below the critical undercooling. In the present study, however, the transition from the metastable YAP to the stable YAG occurred only around the critical cooling rate where the nucleation frequency of YAG is similar to that of YAP. In this case, it is not necessary for YAG to nucleate on the primary YAP and YAG can independently nucleate at the different place in the remaining melt. It is interesting that YAG has already nucleated at the different place from the growing YAP, as shown by arrow in Fig. 7. In the case of the metallic system, once nucleation of the stable or metastable phases occurs, the solid part will sweep throughout the droplet, because the growth velocity of metal is very high, $\sim$m/s. Therefore, it is difficult for another phase to nucleate at different place in the remaining melt even at the same nucleation frequency. On the other hand, in the YAG system, the first nucleation of YAP allows the nucleation of YAG at the different place in the remaining melt, because of the considerably low growth velocity of YAP, $\sim$10 mm/s. The growing YAP was remelted by the latent heat of YAG that was growing almost at the same time and resulted in the microstructure in Fig. 5. Therefore, this recalescence behavior is termed as simultaneous recalescence, not as double recalescence.

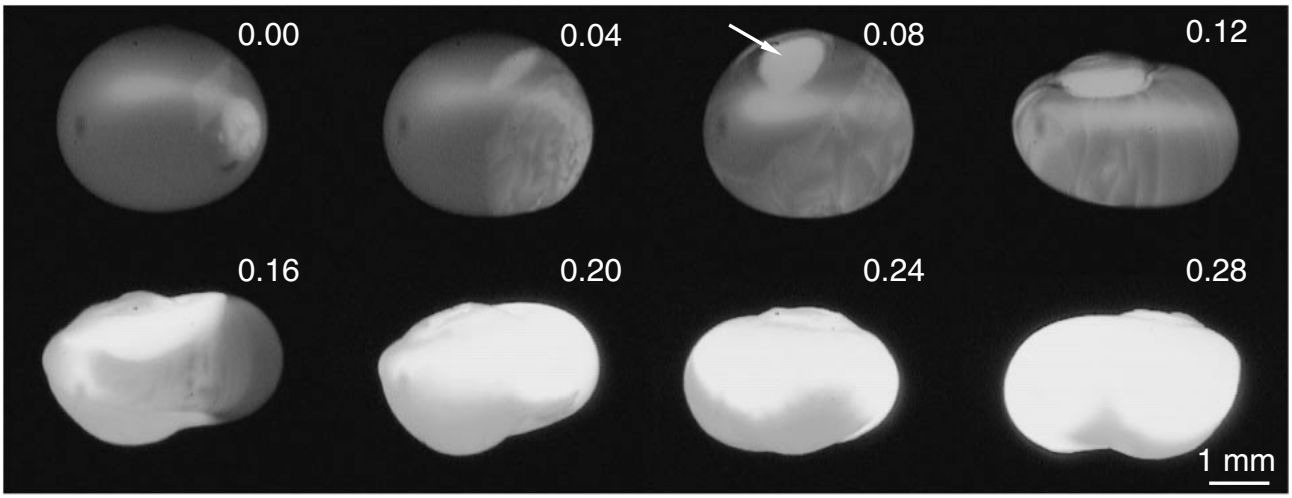

Fig. 7 HSV images of the sample containing both YAP and YAG. The elapsed time (in seconds) is indicated at the top right of the photographs.

4. Summary

Containerless solidification of YAG was carried out using the AAL to elucidate the phase selection condition in the YAG system. Following results was elucidated.

(1) As the cooling rate increased, the metastable mixture of YAP and Al_2O_3, YAG and the amorphous phase were successively obtained. Phase selection in the YAG system depends not on T_{cl} but on the cooling rate.

(2) At the critical cooling rate of approximately 50 K/s for the formation of the metastable mixture and YAG, simultaneous recalescence of YAP and YAG was observed by HSV, and the sample obtained contained both the metastable mixture and YAG. Compare to the well-known double recalescence behavior, metastable YAP and stable YAG can independently nucleate at the different place in the remaining melt, because the nucleation rate of YAG is consistent with that of YAP at the critical cooling rate.

REFERENCES

1) Z. Yongzong: J. Crys. Growth **78** (1986) 31–35.
2) A. Ikesue, T. Kinoshita, K. Kamata and K. Yoshida: J. Am. Ceram. Soc. **78** (1995) 1033–40.
3) Y. Waku, N. Nakagawa, T. Wakamoto, H. Ohtsubo, K. Shimizu and Y. Kohtoku: Nature **389** (1997) 49–52.
4) J. L. Caslavsky and D. J. Viechnicki: J. Mater. Sci. **15** (1980) 1709–1718.
5) M. Gervais, S. LeFloch, J. C. Riffret, J. Coutures and J. P. Coutures: Mat. J. Am. Ceram. Soc. **75** (1992) 3166–3168.
6) Y. Mizutani, H. Yasuda, I. Ohnaka and Y. Waku: Mater. Trans. **42** (2001) 238–244.
7) M. Gervais, S. LeFloch, N. Gautier, D. Massiot and J. P. Coutures: Mater. Sci. Eng. **B45** (1997) 108–113.
8) J. K. R. Weber, D. S. Hampton, D. R. Merkley, C. A. Rey, M. M. Zatarski and P. C. Nordine: Rev. Sci. Instrum **65** (1994) 456–465.
9) K. Nagashio and K. Kuribayashi: Acta Mater. **49** (2001) 1947–1955.
10) K. Nagashio and K. Kuribayashi: Metall. Mater. Trans. A **33A** (2002) 2955–2961.
11) K. Nagashio and K. Kuribayashi: J. Am. Ceram. Soc. **85** (2002) 2550–2556.
12) K. Eckler, F. Gartner, H. Assadi, A. F. Norman, A. L. Greer, and D. M. Herlach: Mater. Sci. Eng. **A226–228** (1997) 410–414.
13) T. Koseki and M. C. Flemings: Metall. Mater. Trans. **26A** (1995) 2991–2999.
14) T. Volkmann, W. Loser and D. M. Herlach: Metall. Mater. Trans. **28A** (1997) 453469.